

International Journal of Scientific Research and Reviews

Particle Size Dependent Ferroelectric, Magnetic and Dielectric Properties of BiFeO₃

S. K. Chavda, P. V. Kanjariya, G. D. Jadav and J. A. Bhalodia*

CMR and HTSC Laboratory, Dept. of Physics, Saurashtra University, Rajkot, 360 005, Gujarat, India

*E-mail: jabrajkot@rediffmail.com

ABSTRACT:

BiFeO₃ (BFO) exhibits ferroelectric and antiferromagnetic behavior simultaneously above room temperature ($T_C \sim 1100$ K, $T_N \sim 643$ K), so it possesses multiferroic behavior. High leakage current and low magnetoelectric coupling at room temperature in BFO limits its applications in spin based electronics - spintronics devices. Synthesis of phase pure BFO has been a challenging task as the product is usually contaminated with the presence of impurity phases like Bi₂Fe₄O₉ and Bi₂₅FeO₃₉. Reduction in leakage current and increment in resistivity can be achieved in BFO by eliminating secondary impurities and oxygen vacancies, i.e. by achieving pure phase of BFO ferroelectric behavior can be improved. We have used Solid State Reaction technique to prepare BFO, the sample was leached using diluted HNO₃ and ball milled using high energy ball miller for 0, 5, 10, 15, 20 and 25 hours to prepare samples with different particle size. Structural properties, particle size dependent P-E loop, M-B loop and Dielectric behavior at room temperature of prepared BFO samples will be discussed in this paper.

KEYWORDS: Multiferroic Materials, Spintronics, Solid State Reaction technique.

***Corresponding Author:**

J. A. Bhalodia*

CMR and HTSC Laboratory,

Dept. of Physics, Saurashtra University,

Rajkot, 360 005, Gujarat, India

*E-mail: jabrajkot@rediffmail.com

INTRODUCTION

Multiferroics are materials that show any two or more ferroic (electric, magnetic (ferro/antiferro/ferri), elastic and toroidic) orders simultaneously in a single phase¹. Magnetoelectric coupling describes the manipulation of magnetic (or electric) field on the polarization (or magnetization) of material, piezoelectric (electrostriction) couples a alteration of strain as a linear function of applied electric field, or change in polarization as a linear function of applied stress, piezomagnetic (magnetostriction) coupling describes a change in strain as a linear function of applied magnetic field, or a change in magnetization as a linear function of applied stress. Magnetoelectric multiferroics, piezoelectric multiferroics and piezomagnetic multiferroics are three main classes based on this phenomenon. The first magnetoelectric multiferroic was discovered by E. Ascher et al. in 1966², but the field remained inactive until 1994 when Hans Schmid coined the term “Multiferroics”. Among all multiferroic materials, magnetoelectric multiferroics are very famous as these materials coexist ferroelectricity and magnetism together. It offers a new aspect in application possibilities in the field of spintronics and magnetic field sensors, being under intense development and an idea of four-state memory^{3,4}.

The most of the multiferroic materials possesses perovskite crystal structure and it can also posses hexagonal or rhombohedrally distorted crystal structure⁵. The ideal structure of perovskite is primitive cubic structure ABO_3 (space group Pmm) with the lattice parameter $a \sim 4 \text{ \AA}$. BFO has a rhombohedrally distorted structure whose magnetic order with a long-periodicity spiral falls in the G-type antiferromagnetic nature below the Neel temperature $T_N = 643 \text{ K}$ and ferroelectricity below $T_{C-FE} = 1100 \text{ K}$ ⁶. The ferroelectricity in $BiFeO_3$ is due to $Bi^{3+} 6s^2$ lone pair while the weak ferromagnetism results from residual moment of the canted Fe^{3+} spin structure⁷. BFO crystallizes in $R3c$ symmetry; here all metal ions are displaced along the (111) direction relative to the ideal centrosymmetric position and the oxygen octahedral surrounds Fe are rotated alternatively around the axis. The technique we used to reduce the particle size of prepared powder sample is mechanical activation or ball milling. It is a top down approach in which a suitable powder charge (typically, a blend of elemental) is placed in a high energy mill, along with a suitable milling medium. The objective of ball milling is to reduce the particle size and unifying particles in new phases. The different type of ball milling can be used for synthesis of nanomaterials in which balls impact upon the powder. Consequently BFO finds use for several applications such as non-volatile information storage, spintronic sensors, wireless sensors, digital memories, spin filters etc.

EXPERIMENTAL SECTION

The conventional Solid State Reaction technique was used to prepare the BiFeO₃ multiferroic material. Figure no. 1 shows the flow chart of synthesis and characterization process. For the synthesis of BFO, 99.95% pure Bi₂O₃ and Fe₂O₃ chemicals of Sigma Aldrich were weighed and mixed, using pestle and mortar. Then in alcoholic medium thoroughly grinding was done for 60 minutes. After that the sample was calcined in the alumina crucible at 650°C for 120 minute, and then the furnace was allowed for natural cooling. The powder sample was once again ground for 120 minute and then sintered at 800 °C for 60 minute^{8,9}. Leaching was done to remove impurity phases, and it was confirmed that impurities were absent in this leached sample by powder XRD pattern.

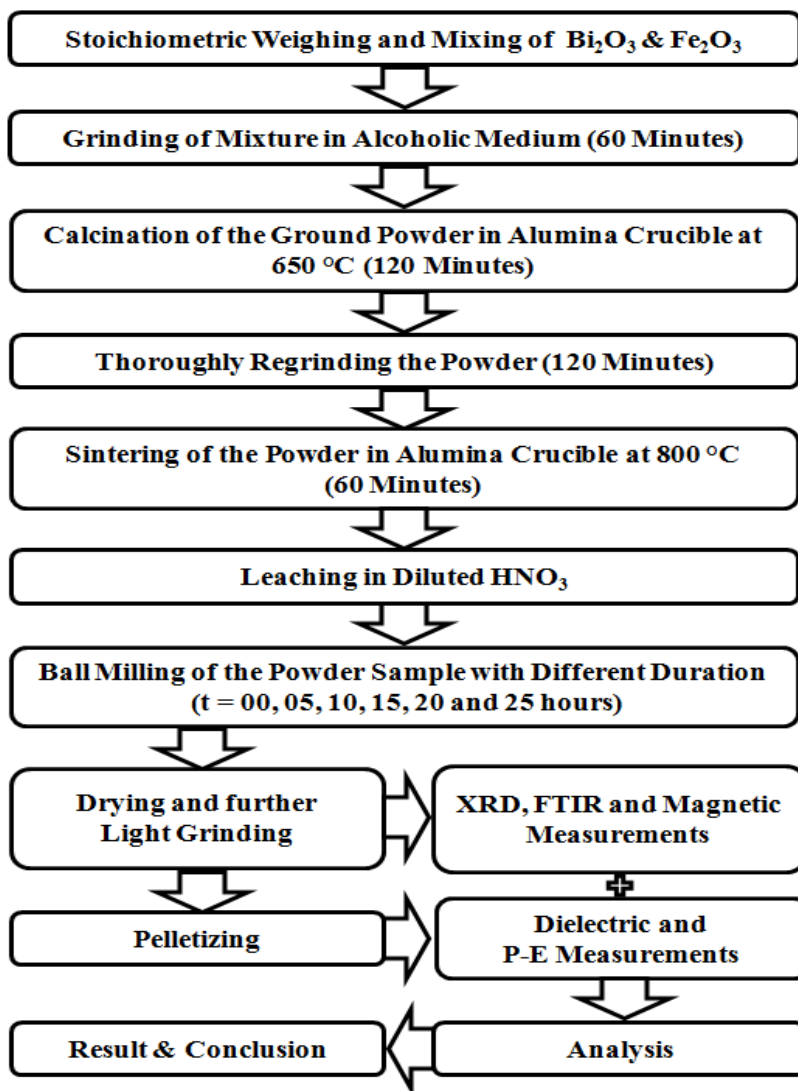


Figure No. 1 : Flow chart for synthesis and characterization of BiFeO₃.

After achieving single phase BFO, ball milling was done using a high-energy planetary ball miller "Pulverisette6" (Fritsch, Germany). In milling, the ball to powder weight ratio was 10:1 and the medium used for milling was HPLC grade H₂O. The time intervals chosen for milling was 05, 10, 15, 20 and 25 hours at 300 RPM and the silicon carbide balls of uniform diameter (5 mm) were used¹⁰. The sample powder of pure single phase BFO was taken and coded as BFO_00, after milling powder samples were coded as BFO_05, BFO_10, BFO_15, BFO_20 and BFO_25. After this, characterizations like XRD, FTIR and M-B loop were carried out for powder samples, whereas dielectric and P-E loop measurements were taken after preparing pellets of all the samples by applying pressure only.

X'Pert Powder PANalytical X-ray diffractometer with *Cu* K-alpha radiation ($\lambda = 1.5405 \text{ \AA}$) was used for this characterization available, the step size was 0.02 degree with total scanning time 30 minute. The XRD patterns of the samples were analyzed using PowderX. The FTIR and M-B loop data were taken for prepared powder forms of all the samples and pellets of the samples were prepared by applying pressure only, for ferroelectric P-E hysteresis loops and dielectric measurements were taken using a ferroelectric hysteresis measurement tester and using impedance analyzer of Agilent, USA, available at Department of Physics, Saurashtra University, Rajkot.

RESULTS AND DISCUSSION

XRD

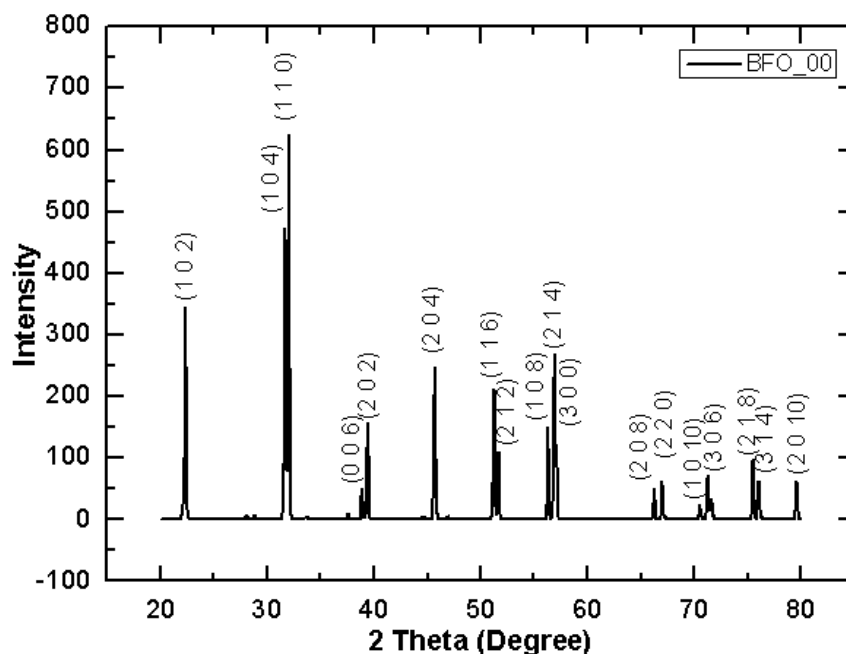


Figure No. 2 : PowderX fitted XRD pattern of BFO_00.

The XRD pattern of figure no. 2 is for BFO_00 or unmilled BFO sample shows the rhombohedrally distorted perovskite structure (with R3c space group) with profile fitting parameters $a = b = 5.57892 \text{ \AA}$, $c = 13.86866 \text{ \AA}$, $\alpha = \beta = 90^\circ$, $\gamma = 120^\circ$ (JCPDS Card No. 86-1518, $a = b = 5.577 \text{ \AA}$, $c = 13.861 \text{ \AA}$, $\alpha = \beta = 90^\circ$, $\gamma = 120^\circ$).

Table No. 1 : Effect of ball milling on particle size and density of the sample.

Sample code	Physical density gm/cm ³	Particle size from Scherer equation (nm)
BFO_00	4.355	65.593
BFO_05	3.350	9.643
BFO_10	3.161	7.078
BFO_15	3.338	14.463
BFO_20	3.350	8.854
BFO_25	3.318	9.344

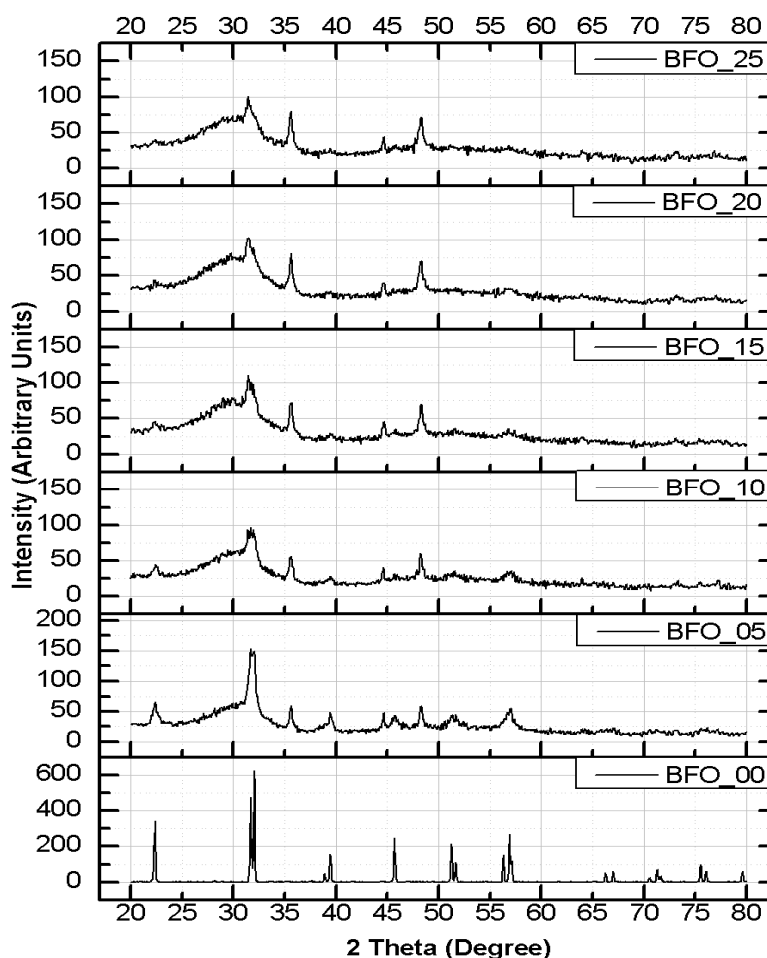


Figure No. 3 : This figure shows the XRD patterns of all the samples, generation of new peak occurs at 35.6° , 45.0° and 48.3° can be seen for all the ball-milled samples.

Figure no. 3 clearly shows that line broadening increases for all peaks and peaks with higher 2θ values (50° to 80°) gets suppressed for ball milled samples, line broadening at 22.4° , 31.72° and 32.05° are easily notable and which results in decreased particle size. As shown in figure no. 3 XRD patterns for BFO show that the line broadening increases as milling duration increases. Another important and notable thing is generation of new peaks at 2θ values of 35.6° , 45.0° and 48.3° in all ball milled samples, profile fitting parameters for newly generated peaks in BFO_05, BFO_10, BFO_15, BFO_20 and BFO_25 are $a = 7.951 \text{ \AA}$, $b = 8.427 \text{ \AA}$, $c = 6.0170 \text{ \AA}$ and $\alpha = \beta = \gamma = 90^\circ$. These peaks are well matching with JCPDS No. 74-1098 of $\text{Bi}_2\text{Fe}_4\text{O}_9$, which is an orthorhombic phase with lattice parameters $a = 7.950 \text{ \AA}$, $b = 8.428 \text{ \AA}$ and $c = 6.005 \text{ \AA}$. and $\alpha = \beta = \gamma = 90^\circ$. Table no. 1 shows the calculated particle size and physical density. Scherer's formula was used to find out particle size. Particle size decreases drastically for ball milled samples and physical density changes as listed in table.

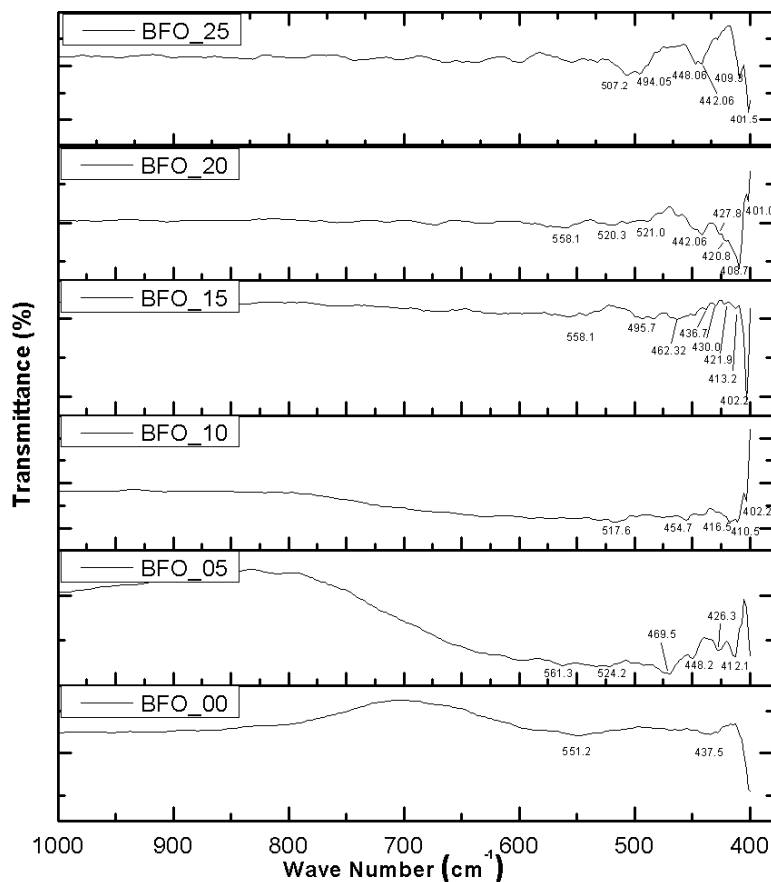


Figure No. 4 : FTIR Spectral response of prepared BFO_00, BFO_05, BFO_10, BFO_15, BFO_20 and BFO_25 at 300 K temperature.

FTIR

Fourier Transform Infrared (FTIR) spectroscopy was done for all the prepared BFO samples and their spectra are as shown in the figure no. 4. It was done over complete FTIR range using KBr as a medium, but as only metal and their derived oxides are present. Peaks in the region 400 cm^{-1} to 800 cm^{-1} are shown in figure no. 4. As shown in the figure no. 4, FTIR spectra of the BFO samples in which two absorption peaks at 550 cm^{-1} and 438 cm^{-1} are characteristic of the Fe–O stretching and bending vibrations of octahedral FeO_6 groups respectively, and implying the formation of BiFeO_3 phase^{7,8}. It can be seen from the graph that as duration of milling increases the absorption increases, compared to large particle size sample. It can be attributed to the nano sized particles of BFO samples, it leads to more surface area and grain boundaries.

DIELECTRIC MEASUREMENTS

Figure no. 5(a) and 5(b) show the dielectric constant and dielectric loss curves for the frequency range of 10 KHz to 2 MHz. It is clear that dielectric constant decreases linearly as $\log f$ increases. Lowest difference of dielectric constant is of 0.8 for BFO_15 sample (at 10 KHz to 1 MHz) and highest is 1.6 for BFO_00 sample. Value of dielectric loss decreases and reaches near to zero as applied frequency increases beyond 1 MHz.

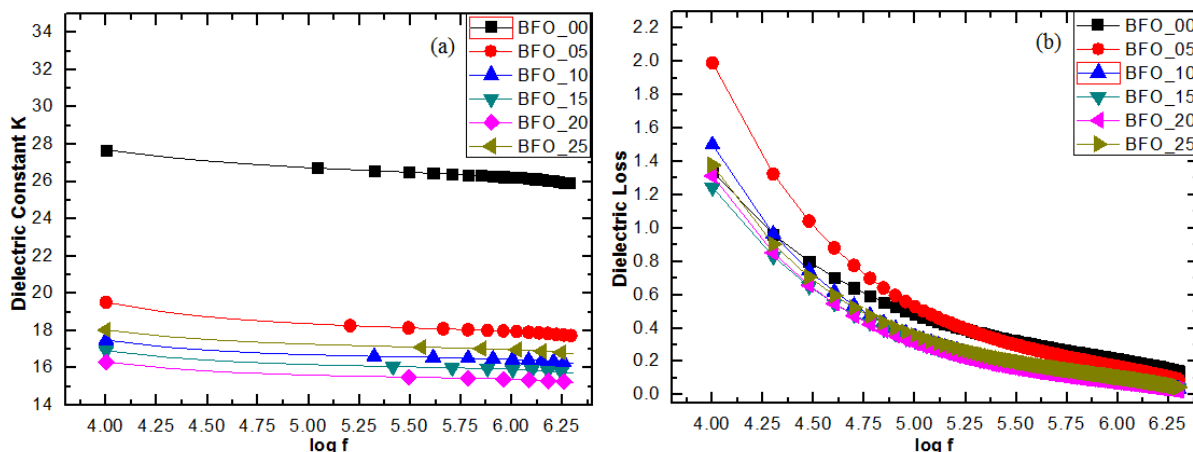


Figure No. 5 : (a) Graph of dielectric constant versus $\log f$, (b) Graph of dielectric loss versus $\log f$.

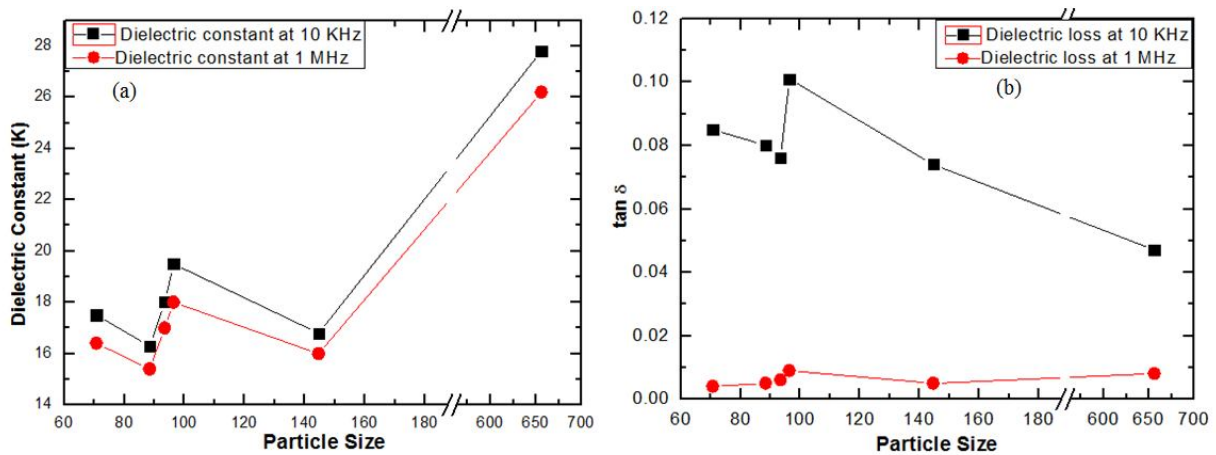


Figure 6 No. : (a) Graph of dielectric constant versus particle size, (b) Graph of dielectric loss versus particle size.

Figure no. 6(a) and 6(b) shows particle size dependent relations of dielectric constant and dielectric loss respectively. Dielectric constants and dielectric loss of all the BFO samples are as listed in the table no. 2. Dielectric loss is highest at low frequencies; table no. 2 gives the values of dielectric loss ($\tan \delta$) at 10 KHz and 1 MHz frequencies. Maximum difference of dielectric loss between 10 KHz and 1 MHz is ~ 0.092 for BFO_05 sample and minimum difference is ~ 0.039 for BFO_00 sample.

Table No. 2 : Dielectric constants and dielectric loss ($\tan \delta$) of BFO samples at 10 KHz and 1 MHz frequencies.

Sample Code	Dielectric Constant		Dielectric Loss ($\tan \delta$)	
	10KHz	1 MHz	10KHz	1 MHz
BFO_00	27.8	26.2	0.047	0.008
BFO_05	19.5	18.0	0.101	0.009
BFO_10	17.5	16.4	0.085	0.004
BFO_15	16.8	16.0	0.074	0.005
BFO_20	16.3	15.4	0.080	0.005
BFO_25	18.0	17.0	0.076	0.006

P-E LOOP MEASUREMENTS

Grain size effects are a major barrier in the miniaturization and applications of ferroelectric ceramics. The ferroelectric P-E hysteresis loops were measured using a ferroelectric hysteresis measurement tester. The ferroelectric loops of all the BFO samples are shown in figure no. 7.

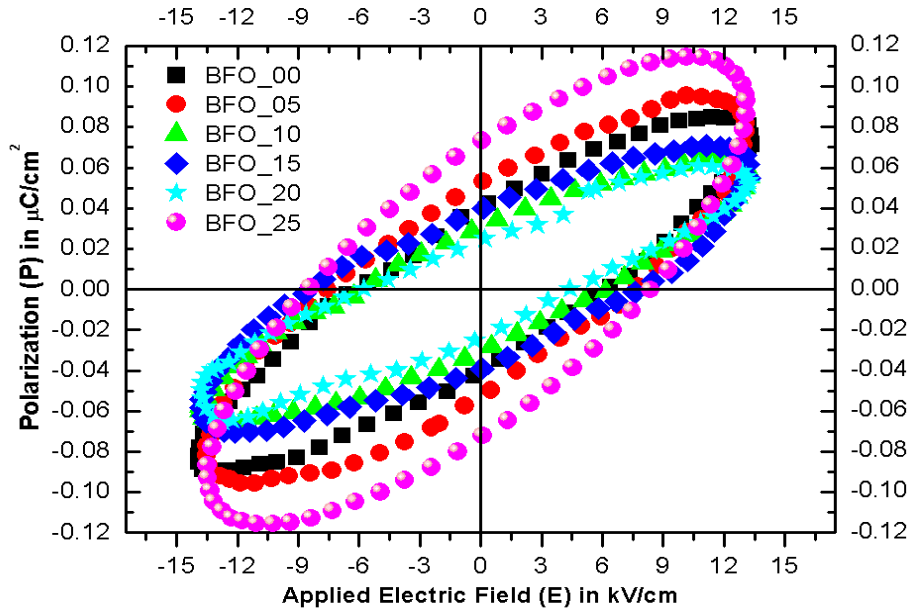


Figure No. 7: P-E Loops of all the samples at room temperature.

These P-E loops are shown in the single plot for direct comparative study of the effect of particle size on ferroelectric behavior of the samples. As shown in loop no any sample has sharp saturation polarization, and there is absence of perfect hysteresis loop. Grain size is one of the important parameter for ferroelectricity or electric hysteresis loop, variation in coercivity, remnant polarization and saturation polarization as a function of varying particle size are depicted in table no. 3. From this table it can be concluded that remnant polarization and coercivity is highest for the sample with particle size ~ 9.34 nm (BFO_25) and lowest for the sample with particle size ~ 8.85 nm (BFO_20).

Table No. 3 : Value of coercivity, remnant polarization and saturation polarization.

Sample Code	Particle size (nm)	Coercivity	Remnant polarization	Saturated polarization
BFO_00	65.593	6.19	0.039	0.087
BFO_05	9.643	7.62	0.054	0.096
BFO_10	7.078	6.07	0.030	0.066
BFO_15	14.463	8.21	0.040	0.070
BFO_20	8.854	5.12	0.025	0.063
BFO_25	9.344	8.46	0.072	0.115

M-B LOOP MEASUREMENT

M-B loops of all the samples are as shown in the figure no.8. BFO is G-type antiferromagnetic by nature and their hysteresis loop does not show good remnant magnetization and coercive values, which can be seen in the figure no. 8. Here B is the applied magnetic field and M is the magnetization within the sample.

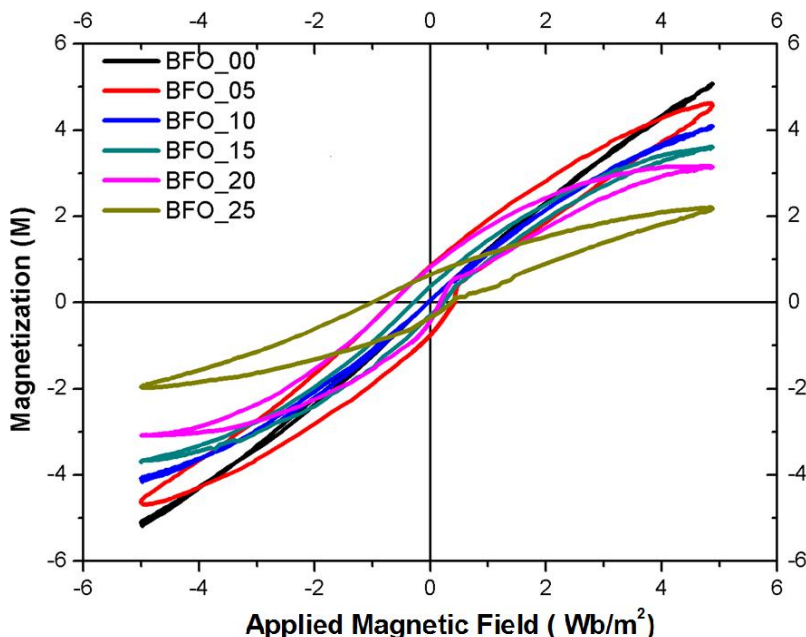


Figure No. 8 : M-B loops of all the samples at room temperature.

From the plots it can be seen that saturation magnetization decreases as milling time increases, this change may be due to breaking of magnetic cycloid of BFO, which was essentially present in BiFeO_3 ⁶. The average saturation magnetization is highest for unmilled BFO (BFO_00) with pure antiferromagnetic behavior. The net remnant magnetization, coercive field values and saturation magnetization relation are tabulated in table no. 4.

Table No. 4 : Value of coercivity, remnant magnetization and saturation magnetization.

Sample Code	Coercivity	Remnant Magnetization	Saturation Magnetization
BFO_00	0.08462	0.00915	5.13305
BFO_05	0.08547	0.01116	4.65462
BFO_10	0.09062	0.01159	4.1237
BFO_15	0.09402	0.0569	3.66141
BFO_20	0.11368	0.1023	3.12527
BFO_25	0.16189	0.21571	2.09233

CONCLUSION

BiFeO₃ powder sample was successfully prepared using solid state reaction technique and particle size dependent physical properties of those samples were characterized and analyzed. XRD characterization has confirmed the synthesis of single phase BiFeO₃ multiferroic material after leaching. There was generation of secondary phase of Bi₂Fe₄O₉ as a result of milling effect. FTIR shows the absence of any organic or other reactions and interestingly more active absorptions regions have taken place in between 560 cm⁻¹ to 400 cm⁻¹ region, the amount of absorption increasing is the result of Fe-O bond modifications. Material with high dielectric constant is good in ferroelectric nature, but unfortunately BiFeO₃ is not having high dielectric constant because leakage current generation takes place around grain boundaries. Among all the samples BFO_00 have highest dielectric constant of about 27.8 at 10 KHz. P-E loop measurements show that the particle size variations do not have impressive effect on their electric polarization. P-E loops show that for the samples that are having high dielectric constant will have smooth P-E loop compared to others. M-B loop study gives some important results, the remnant magnetization and coercive field values continuously increase whereas the saturation magnetization values continuously decrease with increasing milling duration.

ACKNOWLEDGEMENTS:

Authors are thankful to the Departmental UGC-SAP & DST-FIST program for providing the experimental facilities.

REFERENCES:

1. D. Kothari, V. R. Reddy, V.G. Sathe, A. Gupta, A. Banerjee, A. M. Awasthi, *Journal of Magnetism and Magnetic Materials* 2008;320:, 548–552.
2. J. A. Bhalodia et al., *Int. J. Chem. Tech. Res. (IJCRGG)*, 2014;06(3): 2144.
3. M. M. Kumar, V. R. Palkar, K. Srinivas, S. V. Suryanarayan, *Appl. Phys. Lett.* 2000; 76: 27642766.
4. S. K. Chavda, P. V. Kanjariya, G. D. Jadav and J. A. Bhalodia, *Proceedings of RK University's First ICRE*, 2016; 978-93-5254-061-7.
5. G. Felicia, C. Mihai, J. Adelina, M. Valentina, M. Liliana, *Solid State Sciences* 2013;23: 79-87.
6. T. Pathak, Ph. D. Thesis Saurashtra University, 2013.
7. G. V. S. Rao, C. N. R. Rao, J. R. Ferraro, *Appl. Spectrosc.* 24: 436.
8. S. K. Chavda, P. V. Kanjariya, G. D. Jadav and J. A. Bhalodia, *ICRE Proceeding*, ISBN: 978-

93-5254-061-7, 2016;1131-1136.

9. P. V. Kanjariya, S. K. Chavda, G. D. Jadav and J. A. Bhalodia, ICRE Proceeding, ISBN: 978-93-5254-061-7, 2016; 1027-1034.
 10. S. K. Chavda, P.V. Kanjariya, S. J. Sondarva and J. A. Bhalodia, ISSRTST proceeding, ISBN: 978-81-93347-55-3, 2017;1(1): 164-173.
-